
Factor Analysis of Dynamic Series (FADS) in Somatostatin Receptor Imaging

Hélène Kolesnikov-Gauthier, Damien Huglo, Marie Nocaudie and Xavier Marchandise

Department of Nuclear Medicine, Centre Hospitalier Regional et Universitaire of Lille, Lille, France

The aim of this article was to study the physiopathology of tumoral uptake of ^{111}In -pentetretotide using factorial analysis of dynamic series (FADS) and to assess the usefulness of this analysis in somatostatin receptor scintigraphy. **Methods:** Forty-one patients were included, 24 women and 17 men. After intravenous injection of 111 MBq ^{111}In -pentetretotide, dynamic image acquisition (68 images of 30 s) began in front of the suspected tumoral site: thoracic in 10 patients with medullary carcinoma of the thyroid and 2 patients with bronchogenic carcinoid, and abdominal in 12 cases of midgut carcinoid and 17 cases of other gastroenteropancreatic neuroendocrine tumors. FADS was performed with FAMIS software. Static images were obtained 4 h and 24 h later. For every patient, surgery and/or clinical follow-up (4 y) was used to classify results as true (T) or false (F) positive (P) or negative (N) and to evaluate both the sensitivity of static images and the usefulness of FADS. **Results:** Of the 14 cases of carcinoid tumor, 5 patients were TN; 9 patients were TP with static images but only 8 were TP with FADS (a bronchogenic carcinoid of 6 mm was missed). Of the 17 cases of gastroenteropancreatic neuroendocrine tumor, static images were TP in 9 patients, and FADS were TP in 5 of these patients (and 4 FN). Static images and FADS were FN in 4 patients and TN in 3 patients, and in the 2 last patients static images were FP, but FADS were TN. Of the 10 cases of medullary carcinoma of the thyroid, static images and FADS were TN in 1 patient, static images were TP in 3 patients and FADS were TP in 2 of these patients (and 1 FN). In the six last cases, static images were FN, but FADS were FN in 3 patients and TP in 3 patients, showing an infiltrate. **Conclusion:** FADS demonstrates that tumoral kinetics are similar to those of the spleen. FADS can show a diffuse tumoral uptake corresponding to tumoral infiltrate in medullary carcinoma of the thyroid or in hepatic miliaria, whereas static images were normal or doubtful.

Key Words: neuroendocrine tumors; somatostatin receptor imaging; ^{111}In -pentetretotide; factor analysis of dynamic structure; factor analysis of dynamic series

J Nucl Med 1999; 40:33–39

Neuroendocrine tumors are rare tumors that develop from the diffuse endocrine system. They may possess somatostatin receptors (1). Since 1992, imaging these receptors has taken a place of pride among the methods used for diagnosing neuroendocrine tumors, which are difficult to

locate using conventional imaging procedures. Because the curative treatment for these tumors is surgery, it is essential to precisely locate the lesions. Radioisotopic scanning can detect new locations that could imply a change in the therapeutic management (1,2). Scanning is of particular interest in the assessment of multiple endocrine neoplasms and can detect the different kinds of associated lesions (3).

Factorial analysis was derived from correspondence analysis, which is a branch of the statistical analysis of multidimensional data. It has been successfully applied in nuclear medicine to dynamic series (4–12), where it provides a more effective means of study than the regions of interest method (4–7). For some researchers, it is also more effective than Fourier analysis in radioisotopic angiocardigraphy imaging (11). This method provides an automatic way of identifying the pixels in which neighboring temporal changes are occurring. Using factorial analysis, the kinetics of uptake and/or elimination (described by the factorial curve) can be associated with the corresponding structures (represented on the factor image). This method can distinguish between two superimposed structures in a two-dimensional plane, provided they have different uptake kinetics, which is not possible with the regions of interest method.

The aim of this study was to apply factorial analysis to dynamic images performed systematically during ^{111}In -pentetretotide scans to obtain a better understanding of tumor uptake kinetics and to determine the possible usefulness of this technique in analyzing scanning data.

MATERIALS AND METHODS

Patients

Forty-one patients were studied over a period of 2 y: 24 women and 17 men with a mean age of 46 y (range: 11–80 y). The first group was made up of 14 patients examined for a carcinoid tumor or carcinoid syndrome: 8 women and 6 men, with a mean age of 53 y (range: 11–80 y). The second group was made up of 17 patients examined for showing clinical symptoms and/or laboratory test signs suggesting a gastroenteropancreatic neuroendocrine tumor: 11 women and 6 men, with a mean age of 48 y (range: 25–75 y). The third group was made up of 10 patients examined for a known or suspected medullary carcinoma of the thyroid (MCT): 5 women and 5 men, with a mean age of 40.5 y (range: 26–72 y).

The ^{111}In -pentetretotide scan was requested either as part of the diagnostic assessment or because of a suspicion of recurrence. The clinical context and the results of supplementary examinations on patients are summarized in Table 1.

Received Oct. 24, 1997; revision accepted Apr. 28, 1998.

For correspondence or reprints contact: Damien Huglo, MD, Service de Médecine Nucléaire, Hôpital Huriez, CHRU de Lille, 59037 Lille Cedex, France.

TABLE 1
Clinical Context and Results of Supplementary Examinations

Patient				Somatostatin receptor imaging				Therapeutic management and follow-up	
No.	Sex	Age (y)	Clinical context†	Primary tumor	Other known lesions‡	Static images	FADS		FADS + static images
1	F	64	Carcinoid tumor	Small intestine*	Liver	TP	TP	TP	Chemotherapy
2	F	70	Carcinoid tumor	Small intestine*	Liver	TP	TP	TP	Death
3	M	80	Carcinoid tumor	Small intestine	Lungs, liver	TP	TP	TP	Death
4	M	67	Carcinoid tumor	Ileum*	Liver	TP	TP	TP	Chemotherapy
5	M	61	Carcinoid tumor	Small intestine		TP	TP	TP	Hepatic chemoembolization
6	M	55	Carcinoid syndrome	Unknown	Liver	TP	TP	TP	Chemotherapy
7	F	60	Carcinoid tumor	Pancreas*	Liver, bone, lungs	TP	TP	TP	Treated by somatostatin analog
8	M	44	Cushing's syndrome	Bronchus		TP	TP	TP	Cured by surgery (bronchogenic carcinoid: 9 mm)
9	F	45	Cushing's syndrome	Bronchus		TP	FN	TP	Cured by surgery (bronchogenic carcinoid: 6 mm)
10	F	57	Carcinoid tumor	Pancreas	Liver	TN	TN	TN	Surgery: serous cystadenoma, normal liver
11	F	67	Carcinoid tumor	Small intestine*		TN	TN	TN	NED
12	F	11	Carcinoid tumor	Cecal appendix*		TN	TN	TN	NED
13	M	22	Carcinoid tumor	Cecal appendix*		TN	TN	TN	NED
14	F	36	Carcinoid syndrome	Unknown		TN	TN	TN	NED
15	F	49	Gastrinoma	Duodenum*	Liver, lymph nodes of the hilus hepatis	TP	TP	TP	Surgery
16	F	57	Gastrinoma	Pancreas		TP	TP	TP	Surgery
17	F	36	Glucagonoma	Pancreas		TP	TP	TP	Surgery
18	M	32	Multiple-secreting tumor	Pancreas	Hepatic miliaria	TP	TP	TP	Chemotherapy, normal colonoscopy 1 y later
19	M	70	VIPoma	Pancreas	Liver	TP	TP	TP	Chemotherapy
20	F	48	Gastrinoma	Stomach		TP	FN	TP	Surgery
21	F	75	Gastrinoma	Pancreas		TP	FN	TP	Surgery
22	M	36	Glucagonoma	Pancreas*	Liver	TP	FN	TP	Chemotherapy
23	M	68	Somatostatinoma	Pancreas*	Abdominal nodes	TP	FN	TP	Treated by somatostatin analog, surgery 3 y later
24	F	39	Gastrinoma	Duodenum	Abdominal lymph nodes	FN	FN	FN	Surgery
25	M	45	Gastrinoma	Duodenum		FN	FN	FN	Surgery
26	F	40	Gastrinoma	Pancreas		FN	FN	FN	Surgery refused by patient
27	F	25	Multiple-secreting tumor	Pancreas		FP + FN	TN + FN	FP + FN	Surgery
28	F	58	Gastrinoma	Pancreas*		FP	TN	FP	No lesion at surgery
29	F	52	Gastrinoma	Duodenum*	Pancreatic lymph nodes	TN	TN	TN	NED
30	M	34	Glucagonoma	Pancreas*		TN	TN	TN	NED
31	F	54	Glucagonoma	Pancreas*		TN	TN	TN	NED
32	F	38	MCT	Thyroid*	Right adrenal	TP	TP	TP	Increase of calcitonin level
33	F	72	MCT	Paratracheal mass		TP	TP	TP	Surgery
34	F	46	MCT	Thyroid*		TP	FN	TP	Calcitonin level increased but stable, NED
35	M	29	MCT	Thyroid*	Bone, lungs, mediastinum, liver	FN	FN	FN	Death
36	M	33	MCT	Thyroid*		FN	FN	FN	Calcitonin level increased but stable, NED
37	M	26	MCT	Thyroid*	Liver, bone	FN	FN	FN	Lost to follow up
38	M	27	MCT	Thyroid*	Adrenals, right paracarotid mass, pulmonary miliaria	FN	TP	TP	Surgery for pheochromocytomas, hepatic miliaria

TABLE 1 (continued)
Clinical Context and Results of Supplementary Examinations

		Patient				Somatostatin receptor imaging			
No.	Sex	Age (y)	Clinical context†	Primary tumor	Other known lesions‡	Static images	FADS	FADS + static images	Therapeutic management and follow-up
39	F	55	MCT	Thyroid*	Infiltration of the larynx	FN	TP	TP	Palliative surgery
40	M	37	MCT	Thyroid*	Bone, infiltrative tumor	FN	TP	TP	Chemotherapy
41	F	42	MCT	Thyroid*		TN	TN	TN	NED, calcitonin level at the upper limit of normal values
TOTALS									
14 patients			Carcinoid tumors			9 TP, 5 TN	8 TP, 1 FN, 5 TN	9 TP, 5 TN	
17 patients			Gastroenteropancreatic neuroendocrine tumors			9 TP, 4 FN, 2 FP, 3 TN	5 TP, 8 FN, 5 TN	9 TP, 4 FN, 2 FP, 3 TN	
10 patients			MCT			3 TP, 6 FN, 1 TN	5 TP, 4 FN, 1 TN	6 TP, 3 FN, 1 TN	

*Patient surgically treated before somatostatin receptor imaging.
†Clinical context and tumoral type according to biological data, and histology if surgery performed.
‡Other lesions known from conventional imaging or from histology.
FADS = factorial analysis of dynamic series; TP = true positive; TN = true negative; FP = false positive; FN = false negative; NED = no evolutive disease; MCT = medullary carcinoma of the thyroid.

Imaging

Dynamic image acquisition began for each patient during the intravenous injection of at least 111 MBq (111–185 MBq) ¹¹¹In-pentetreotide (OctreoScan; Mallinckrodt, Evry, France). A Sopa DS 7 gamma camera (Sopa Medical Vision, Buc, France) equipped with a high-resolution, medium-energy collimator was centered on the suspected tumor region (thoracic for MCT and bronchogenic carcinoids, abdominal for midgut carcinoids and gastroenteropancreatic neuroendocrine tumors). The dynamic images (matrix 64 × 64) consisted of a series of 68 images, taken every 30 s (i.e., a study duration of 34 min).

The study continued with a whole-body scan during the fourth hour in the form of a series of images centered on the trunk from anterior and posterior views (600 s, 512 × 512 pixels) and a second whole-body scan at 24 h using a Sopa DSX gamma camera (scanning 8 cm/min) and static images centered in the same positions as previous ones.

Data Processing

The dynamic series was analyzed with FAMIS software (Sopa Medical Vision), using the algorithm developed by Barber (5) as modified by Frovin et al. (7). In a healthy patient, a factorial analysis will, depending on the number of factors studied, find one or two vascular factors, a tissue factor and one or more urinary factors corresponding to the elimination of the tracer.

Masks were applied to eliminate vascular activity (cardiac or subclavian) and urinary activity (renal, vesical and sometimes urethral), which accounted for one or more factors without contributing any information value. The masking of these regions made the kinetics of less active trixels more visible and therefore revealed regions of low activity that had unusual kinetics. Suitable masks made the hepatic and splenic kinetics appear distinctly.

Interpretation of the Examinations

All the images of the factorial analysis were examined jointly by the four authors after interpretation of the static images.

Radioisotopic Scans. The pituitary gland, salivary glands, thyroid, liver, spleen, kidneys and the urinary tract physiologically take up or absorb the tracer. Mammary uptake may also be observed. The gallbladder is sometimes visible. Fixation was considered pathological if it occurred outside the above-mentioned organs. The early nature of uptake on the dynamic images had to be associated with a durable nature, persisting on late images. An abnormal intensity of uptake by an organ that normally takes up the tracer and a heterogeneity of uptake within one of these organs, persisting on late images, also was considered pathological.

Factorial Analysis of Dynamic Series. A search was systematically made for two to five factors. A focus visible on the factor image characterized by increasing uptake was interpreted as abnormal when it had the same location as a focus visualized in another manner. When a diffuse activity was visible on the same factor image, it was interpreted as abnormal, even if static images were normal.

The final interpretation of the somatostatin receptor imaging was considered positive when factorial analysis of dynamic series (FADS) or static images were positive (logical combination «or»).

RESULTS

Examinations were classified as true (T) or false (F) and positive (P) or negative (N) relative to the results of surgery and/or monitoring of the outcome (more than 2 y with a mean value of 4 y). The results are shown in Table 1. There were 18 cases of gastroenteropancreatic neuroendocrine

tumors, the results of the scan (static images) in patient 27 being both FP and FN.

When the spleen was in the field of view of the gamma camera, the foci detectable by FADS all appeared on the same factor image as the spleen (Figs. 1 and 2).

Carcinoid Tumors

Of the 14 patients with a known or suspected carcinoid tumor, 5 examination results were TNs (patients 10–14); these cases included 3 postoperative examinations (patients 11–13), 1 suspected carcinoid not confirmed after 3 y of monitoring (patient 14) and a serous cystadenocarcinoma of the pancreas (patient 10). In the remaining patients (patients 1–9), tumors were visualized by radioisotopic scanning (Figs. 1 and 2), including two bronchogenic carcinoid tumors less than 1 cm in diameter (patients 8 and 9). In 1

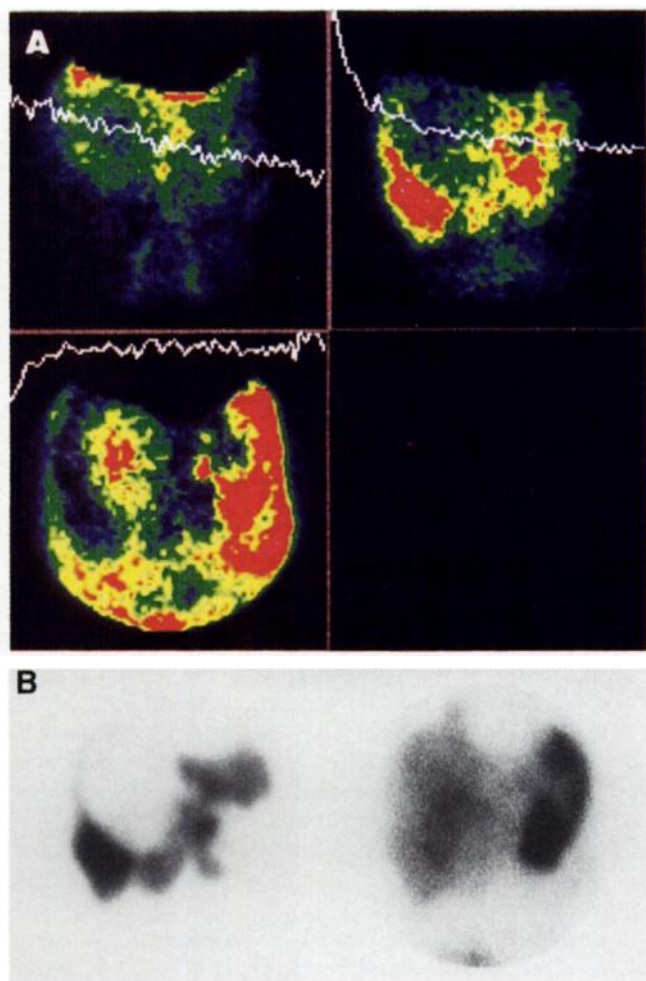


FIGURE 1. Patient 3: FADS was performed with three factors and thoracic mask. (A) First factorial curve (top left) corresponds to vascular activity, and second factorial curve (top right) to hepatic activity (see the analogy with normal hepatic imaging with ^{99m}Tc -phytates, Fig. 1B, left). On last factor image (bottom left, corresponding to splenic and tumoral kinetics), spleen and two big hepatic metastases are seen (right lobe and left lobe). (B) Lesions are seen 24 h later on anterior abdominal image of somatostatin analog imaging (right), corresponding to lack of uptake of normal hepatic functional tracer (^{99m}Tc -phytates, left).

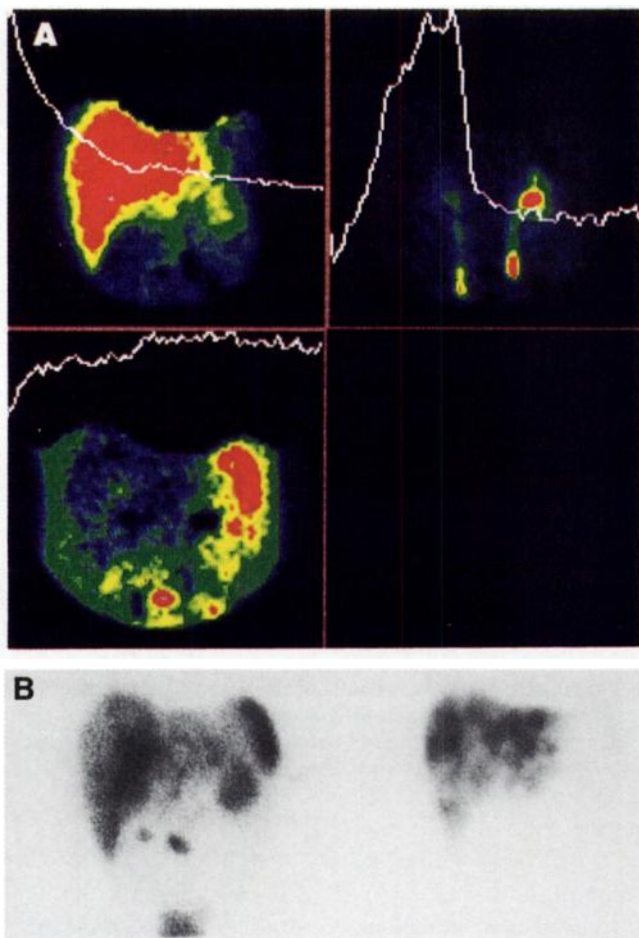


FIGURE 2. Patient 6: FADS was performed with three factors and thoracic mask. (A) First factorial curve (top left) shows a normal hepatic activity, and second factorial curve (top right) shows urinary kinetics. On last factor image (bottom left, corresponding to splenic and tumoral kinetics), spleen, abdominal lesions and hepatic metastases are seen. (B) Twenty-four hours later, on abdominal anterior images, abdominal lesions are clearly seen on somatostatin receptor imaging (left), but hepatic metastases are better seen with comparison of this image and normal hepatic imaging (^{99m}Tc -phytates, right).

patient with polycystic renal and hepatic disease, the scan provided better diagnostic information than conventional imaging by recognizing metastases within the cysts. In 1 patient with bone metastases (patient 7), the ^{111}In -pentetreotide scan enabled an assessment to be made of the lesions, whereas standard bone scans were negative. The sensitivity of the examination was therefore 100% (9/9).

Of the 9 tumors with positive results on static images, 8 were visualized by FADS. FADS was negative in 1 case (patient 9 had a 6-mm-diameter tumor).

Gastroenteropancreatic Neuroendocrine Tumors

Of the 17 patients with gastroenteropancreatic neuroendocrine tumors, 3 examination results were TN; these cases consisted of 2 postoperative check-ups (patients 29 and 30) and 1 suspected glucagonoma (patient 31), still unconfirmed after 4 y of follow-up. In 4 patients, the scans were FNs; a

duodenal gastrinoma of 6 mm (patient 25), a duodenal gastrinoma with lymphatic metastases (patient 24), an immunolabeled multiple-secreting pancreatic tumor (patient 27) and a tumor attributed to Zollinger-Ellison syndrome (patient 26) without surgical intervention and with a pancreatic nodule of 1.3 cm on endoscopic ultrasonography but negative results from a CT scan and nuclear MRI. Two examination results were FPs. In patient 28, who had a history of malignant gastrinoma with surgery 6 y before and persistently abnormal laboratory test results, both the radioisotopic scan and endoscopic ultrasonography detected an abdominal focus, whereas the CT scan results were normal. The surgical findings were negative, and the patient showed no progressive disease 2 y later. Patient 27 had a pancreatic tumor visible by CT scan and undetectable by radioisotopic scanning; the technique therefore gave a FN. There was, however, a clear hyperfixation above the gallbladder that persisted at the 4th and 24th h and that was considered pathological. This localization was not confirmed surgically, so this was FP. The sensitivity of the examination was 69% (9/13).

In 9 cases (patients 15–23), the radioisotopic scan results were positive and detected the tumor sites. Of the 9 patients in whom the tumor could be identified on static images, 5 had positive results with FADS (patients 15–19) and 4 had negative results (patients 20–23). The FADS results were negative in the other patients. In patient 27, the FADS results were therefore both FN (for the undetected pancreatic tumor) and TN (for the fixation above the gallbladder visualized on the static images).

Medullary Carcinoma of the Thyroid

The radioisotopic scanning results using ^{111}In -pentetreotide were positive in 3 of 10 patients (patients 32–34) examined for MCT. The FADS results were positive in 2 of the 3 patients with positive scan results (patients 32 and 33) and negative in patient 34. In 3 patients with local invasion (patients 38–40), the scan results were negative in the mediastinal region, but the FADS showed a diffuse cervical fixation. The FADS results were negative in all other patients. In 2 patients (patients 35 and 37), bone and hepatic metastases were known and the results of a bone radioisotopic scan were positive. The results of the radioisotopic scan with ^{111}In -pentetreotide were negative in these 2 patients. Patient 35 had mediastinal lymph nodes detectable by CT and FADS, and the results could therefore be considered FN. A series of dynamic images centered on the pelvis were conducted on patient 37 because bone metastases were known to exist at this level. The FADS results in this patient were FN. The sensitivity of the static radioisotopic scan images alone was therefore 33% (3/9), and the sensitivity of the whole radioisotopic scan (FADS and static images) was 66% (6/9).

DISCUSSION

Kinetics of Tumor Fixation Similar to Those of the Spleen

All the tumors studied had the same uptake kinetics as the spleen (Figs. 1–3). It is interesting to notice that normal liver, for instance, is not seen on the same factor image as spleen and tumor (Figs. 1 and 2). Autoradiograph techniques

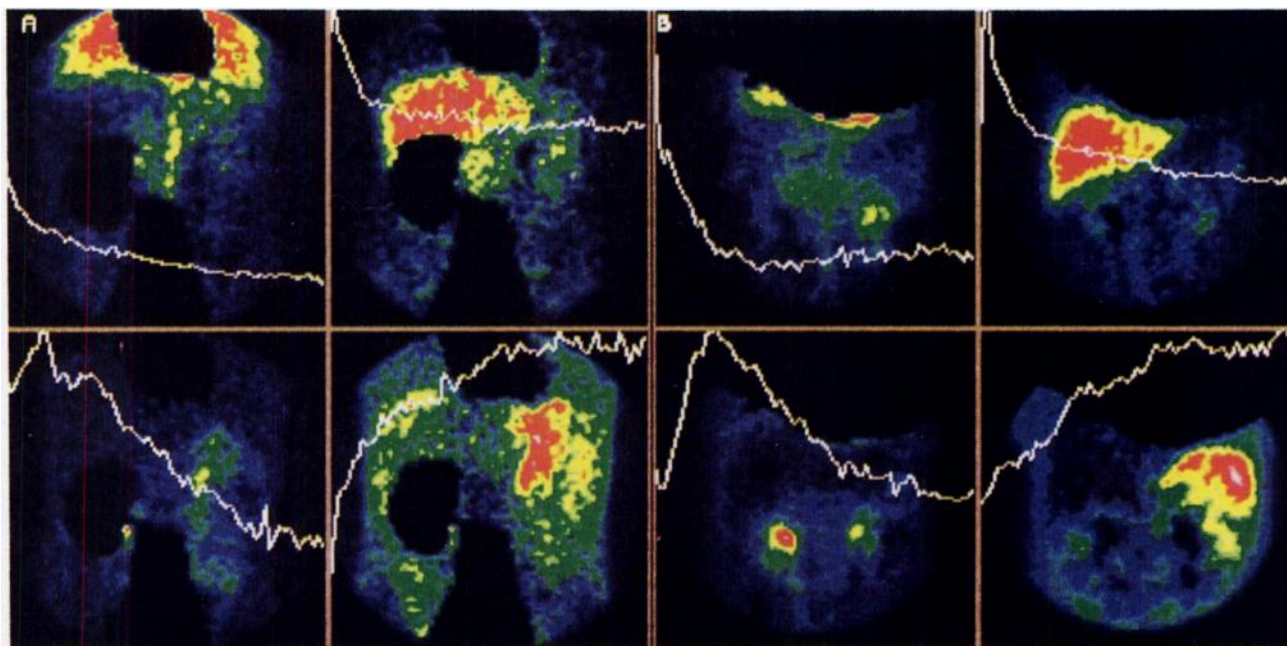


FIGURE 3. Patient 18 with hepatic miliary (A) and patient 30 with normal (TN) study (B): FADS was performed with four factors and cardiac and urinary masks. In both cases, first factorial curve shows vascular activity, second factorial curve a normal hepatic activity and third factorial curve urinary kinetics. On last factor image, corresponding to splenic kinetics, tumoral uptake in hepatic area is seen only for patient 18.

have shown that somatostatin receptors are expressed in normal spleen tissue (13), and the spleen is known to be a target tissue of ^{111}In -pentetreotide. These receptors are mainly localized in the red pulp, but the exact cell type having the somatostatin receptors is unknown (13,14). It seems that it may be the lymphocytes (15). The most likely hypothesis is that spleen uptake is great and remains stable with time because of the presence of many lymphocytes that have somatostatin receptors. Tumors that also have somatostatin receptors can have the same uptake kinetics.

The general form of the factorial curve for the spleen is of the type $y(t) = A(1 - e^{-t/\alpha})$, where A is the height of the plateau, t is time and α is the time constant. In most cases, the form of the curve is slightly different, either because there is the beginning of a decrease after a maximum, which may indicate that the factor does not belong entirely to the spleen but may contain information coming from other tissues (e.g., renal), or that there is a large activity right from the start, so that it is impossible to trace the curve back to the origin. (The first image takes 30 s to capture, and the arrival of the bolus of radioactivity during the 30 s of the first image can vary from one patient to another.) We calculated the value of the time constant after exponential fitting of the curve and deduction of the time needed to reach half-maximum uptake by the spleen (or tumor), $C_{1/2}$. The mean value for $C_{1/2}$ was 2.67 min (± 1.39 SD; range 0.54–5.5 min). Uptake by the spleen and by tumors therefore appeared to be a very rapid phenomenon that occurred in the first few minutes after injection.

Combination of Static Images and FADS Provides Some Increased Sensitivity

Factorial images are often difficult to interpret and it is necessary to use later images, especially for small-sized tumors. In fact, very small anomalies that can correspond to tumor sites can have the same intensity (i.e., the same contribution to the factorial curve) as other pixels corresponding to nonpathological sites. Images were superimposed to ensure that anomalies corresponded in position.

In certain cases, FADS can increase the sensitivity of radioisotopic scans (16). For example, in the three cases of MCT with local invasion, the FADS showed a diffuse appearance of uptake in the cervical region, with a factorial curve corresponding to spleen kinetics. This appearance was never observed in other patients. The static images were described as normal. It is likely that tumor infiltration and/or secondary inflammatory phenomena (with the presence of lymphocytes) were responsible for this special appearance. Similarly, in a case of hepatic miliaria, in which the static images showed a nonuniform hepatic uptake of ^{111}In -pentetreotide, the FADS clearly showed a diffuse hepatic uptake appearance on the image corresponding to the spleen factorial curve (Fig. 3). FADS resulted in an increase in sensitivity from 33% to 66% in the examination for MCT.

Difficulties in Interpreting Factorial Images

FADS can be performed easily, without any irradiation or lengthening of scan duration. Nevertheless, the technique is limited to the field of view of the gamma camera and, if no specific region is under suspicion, the method may fail.

In this study, there are several other possible explanations for the FN results as determined by FADS. The first is the projection of the tumor site onto the position of a kidney (patient 18), making it impossible to produce the renal masks required for creating two different factorial images for the liver and spleen, or making the interpretation tricky because of the constant presence of renal parenchyma on the factor image of the spleen. (The site visualized then corresponds either to the tumor site or to the kidney.) The display of renal parenchyma on the factor image of the spleen varies from one patient to another, probably in relation to the speed at which the tracer is eliminated and on phenomena of tubule reabsorption (17–19).

The small size of the tumor and/or the low density of somatostatin receptors can be another cause of failure (patients 13, 23 and 38) because the matrix for the acquisition of dynamic series was only 64×64 , compared to a matrix of 512×512 for the centered static images (the 6-mm carcinoid tumor was not identified on the whole-body image, only on the centered static image). Dynamic imaging using a finer matrix would undoubtedly resolve this problem, at least in part.

Finally, it is possible that individual factors—such as the existence of ascites, peritoneal carcinosis, renal failure or hydroelectric disorders—could disrupt tracer metabolism (patient 31) and lead to a large background noise, thus making the factorial analysis difficult to interpret.

CONCLUSION

FADS is a useful tool in nuclear medicine for understanding the uptake kinetics of injected tracers. It can be used to identify the special kinetics of tumors that were identical to spleen uptake for all the kinds of tumors that were studied, irrespective of whether they were primary or secondary.

FADS can help interpret images taken late after injection in difficult cases and help confirm the correspondence between a possible cancerous lesion and its presence on the factor image corresponding to a spleen-type curve.

In the case of diffuse lesions (invasive MCT or hepatic miliaria), in which late images can be normal, FADS can provide diagnostic information in addition to that provided by static images by showing diffuse uptake on the spleen type factor image.

ACKNOWLEDGMENTS

We thank the physicians of the services of Endocrine Surgery (Prof. Proye), Endocrinology (Profs. Delcoux, Lefevre and Wemeau) and Gastroenterology (Prof. Paris) of the CHRU of Lille.

REFERENCES

1. Krenning EP, Kwekkeboom DJ, Bakker WH, et al. Somatostatin receptor scintigraphy with (¹¹¹In-DTPA-D-Phe¹)- and (¹²³I-Tyr³)-octreotide: The Rotterdam experience with more than 1000 patients. *Eur J Nucl Med*. 1993;20:716-731.
2. Jamar F, Fiasse R, Leners N, Pauwels S. Somatostatin receptor imaging with Indium-111-pentetreotide in gastroenteropancreatic neuroendocrine tumors: safety, efficacy and impact on patient management. *J Nucl Med*. 1995;36:542-549.
3. Dorr U, Franck-Raue K, Raue F, et al. The potential value of somatostatin receptor scintigraphy in medullary thyroid carcinoma. *Nucl Med Commun*. 1993;14:439-445.
4. Hannequin P, Liehn JC, Valeyre J. Analysis of image sequences in nuclear medicine. #2. Application of factor and analysis methods [in French]. *J Med Nucl Biophys*. 1989;13:125-137.
5. Barber DC. The use of principal components in the quantitative analysis of gamma camera dynamic studies. *Phys Med Biol*. 1980;25:283-292.
6. Houston AS, MacLeod MA, Sampson FD. Principal components analysis as an aid to classification of renal dynamic studies. *Eur J Nucl Med*. 1979;4:295-299.
7. Frouin F, Bazin JP, Di Paola R. FAMIS: A software package for functional feature extraction from biomedical multidimensional images. *Comput Med Imaging Graph*. 1992;16:81-89.
8. Nijran KS, Barber DC. Factor analysis of dynamic function studies using a priori physiological information. *Phys Med Biol*. 1986;31:1107-1117.
9. Samal M, Surova H, Karny M, Marikova E, Michalova K, Dienstbier Z. Enhancement of physiological factors in factor analysis of dynamic studies. *Eur J Nucl Med*. 1986;12:280-283.
10. Bénali H, Buvat I, Frouin F, Bazin JP, Di Paola R. A statistical model for the determination of the optimal metric in factor analysis of medical sequences (FAMIS). *Phys Med Biol*. 1993;38:1065-1080.
11. Cavailloles F, Bazin JP, Di Paola R. Factor analysis in gated cardiac studies. *J Nucl Med*. 1984;25:1067-1079.
12. Lamas-Olier A, Giammarile F, Frouin F, et al. Factor analysis for the study of the initial biodistribution of labeled octreotide [Abstract in French]. *Med Nucl*. 1994;18:238.
13. Krausz Y, Shibley N, De Jong RBJ, Yaffe S, Glaser B. Gallbladder visualization with In-111-labeled octreotide. *Clin Nucl Med*. 1994;19:133-135.
14. Bell GI, Yasuda K, Kong H, et al. Molecular biology of somatostatin receptor. In: *Somatostatin and Its Receptors (Ciba Foundation Symposium 190)*. Chichester, United Kingdom: John Wiley and Sons; 1995:65-88.
15. Bakker WH, Krenning EP, Reubi JCP, et al. In vivo application of (¹¹¹In-DTPA-D-Phe¹)-octreotide for detection of somatostatin receptor-positive tumors in rats. *Life Sci*. 1991;49:1593-1601.
16. Kolesnikov-Gauthier H, Huglo D, Nocaudie M, Marchandise X. Factor analysis of dynamic structures applied to somatostatin receptor imaging in the diagnosis of medullary thyroid carcinoma [in French]. *Med Nucl*. 1997;21:219-225.
17. Bajc M, Palmer J, Ohlsson T, Edenbrandt L. Distribution and dosimetry of ¹¹¹In DTPA-D-Phe¹-octreotide in man assessed by whole body scintigraphy. *Acta Radiol*. 1994;35:53-57.
18. Bong SB, Vanderlaan JG, Louwes H, Schuurman JJ. Clinical experience with somatostatin receptor imaging in lymphoma. *Semin Oncol*. 1994;21(suppl 13):46-50.
19. Krenning EP, Bakker WH, Kooij PPM, et al. Somatostatin receptor scintigraphy with ¹¹¹In-DTPA-D-Phe¹-octreotide in man: metabolism, dosimetry and comparison with Iodine¹²³-Tyr-3-octreotide. *J Nucl Med*. 1992;33:652-658.